Supporting Information

Wang et al. 10.1073/pnas.1305438111

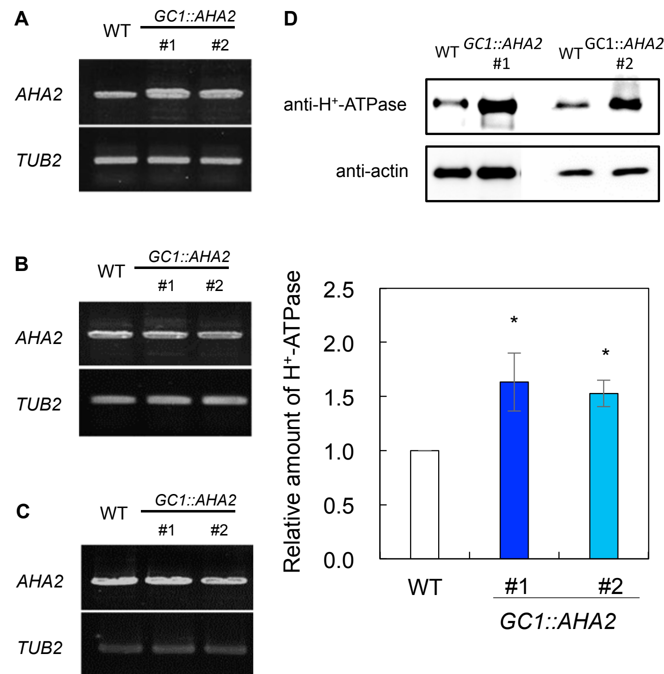

Fig. S1. Reverse transcription–PCR (RT-PCR) and immunoblot analysis of *AHA2*-transgenic plants. (*A*–*C*) RT-PCR analysis of *AHA2* in wild-type (WT) and two *AHA2*-transgenic lines (*GC1::AHA2* #1 and #2) in epidermal tissue (*A*), leaves (*B*), and roots (*C*). *TUBULIN BETA CHAIN2* (*TUB2*) was used as a control. (*D*) Immunoblot analysis was performed according to a previous method (1) with modifications. The epidermal fragments were homogenized in an ice-cold homogenization buffer using a mortar and pestle. The homogenate was solubilized by adding a half-aliquot of SDS sample buffer. The solubilized sample was centrifuged at 12,000 × *g* for 1 min, and the resulting supernatant was subjected to SDS/PAGE. Polyclonal antibodies raised against the catalytic domain of *Arabidopsis AHA2* were described previously (1). Actin protein was detected using anti-actin antibody as a control. The relative amount of H^+-ATPase was quantified as the ratio of H^+-ATPase to actin signal intensity. Values are means ± SEM ($n = 3$ independent experiments). Significant differences were detected by Student *t* test ($*P < 0.05$).

1. Hayashi M, Inoue S, Takahashi K, Kinoshita T (2011) Immunohistochemical detection of blue light-induced phosphorylation of the plasma membrane H^+-ATPase in stomatal guard cells. *Plant Cell Physiol* 52(7):1238–1248.

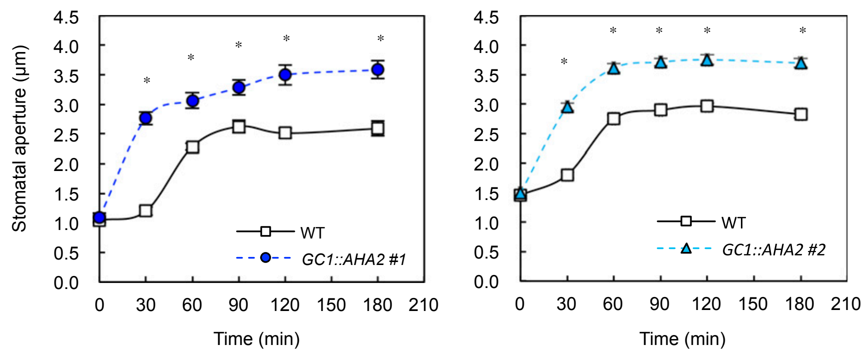

Fig. S2. Time course of stomatal aperture under light (50 μmol·m^{-2}·s^{-1} red light and 10 μmol·m^{-2}·s^{-1} blue light). *GC1::AHA2* #1 (left panel) or #2 (right panel) was compared with the WT, respectively. Stomatal aperture values are the means of measurements of 25 stomata; error bars represent the SEM. Significant differences in stomatal aperture were detected using Student *t* test (*$P < 0.001$).

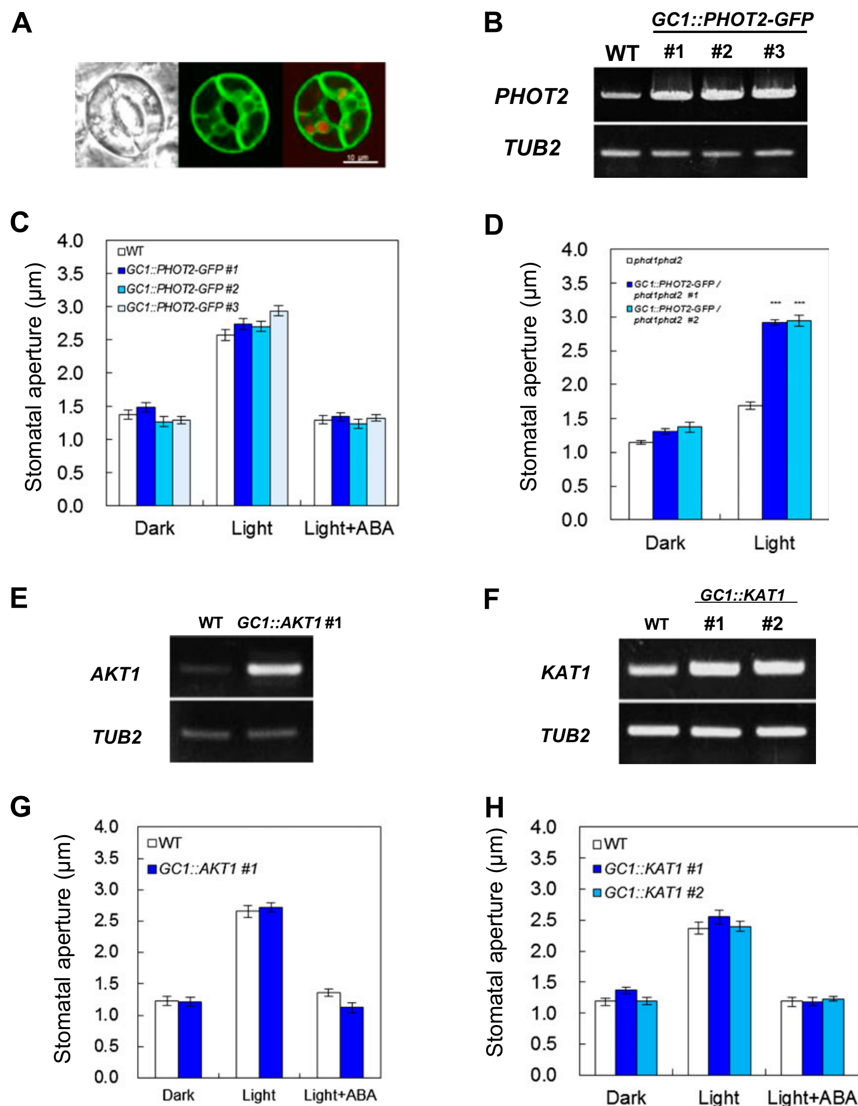

Fig. S3. Overexpression of *PHOTOTROPIN 2* (*PHOT2*)*-GFP*, *ARABIDOPSIS K^{+} TRANSPORTER 1* (*AKT1*), or *POTASSIUM CHANNEL IN ARABIDOPSIS THALIANA 1* (*KAT1*) using the *GC1* promoter had no effect on stomatal opening. (*A*) Bright-field and fluorescent images of typical stomata from *GC1::PHOT2-GFP*. (*B*, *E*, and *F*) RT-PCR analyses of *PHOT2*, *AKT1*, *KAT1*, and *TUB2* in the WT and the transgenic plants *GC1::PHOT2-GFP*, *GC1::AKT1*, and *GC1::KAT1*. *TUB2* was used as a control. (*C*, *G*, and *H*) Stomatal apertures under 2.5 h of darkness, light (red light of 50 μmol·m^{-2}·s^{-1} and blue light of 10 μmol·m^{-2}·s^{-1}), or light in the presence of 20 μM abscisic acid (ABA). (*D*) Stomatal apertures of the *phot1 phot2* double mutant and *GC1::PHOT2-GFP/phot1 phot2* transgenic plants under darkness or 2.5-h light treatment. The light conditions were the same as in *C*. *PHOT2-GFP* restored light-induced stomatal opening in *phot1 phot2*. Stomatal apertures are the means of measurements on 25 stomata; error bars represent the SEM. Differences in stomatal aperture were detected using Student *t* test (***$P < 0.001$).

Fig. S4. Drought tolerance in WT and *AHA2*-transgenic plants. Both WT and *AHA2*-transgenic plants grown in the same planter for 2 wk (*A*) were subjected to drought stress by withholding water for 4 wk (*B*) and for 6 wk (*C*). Six-week-old plants were photographed after the removal of inflorescences.

Fig. S5. Productivity of *AHA2*-transgenic plants. (*A*) Phenotypes of WT and *AHA2*-transgenic line #2 plants grown under high light conditions (200 $\mu mol \cdot m^{-2} \cdot s^{-1}$) for 45 d. (*B*) Dry siliques of WT or *AHA2*-transgenic line #2 plants (*GC1::AHA2* #2). (*C*) Relative average number of siliques per plant. (*D*) Relative average silique dry weight per plant calculated as the total silique dry weight of each plant divided by total silique number of each plant. Silique number and dry weight values are the means of measurements of three plants; error bars represent the SD. Significant differences were detected by Student *t* test (*$P < 0.05$).

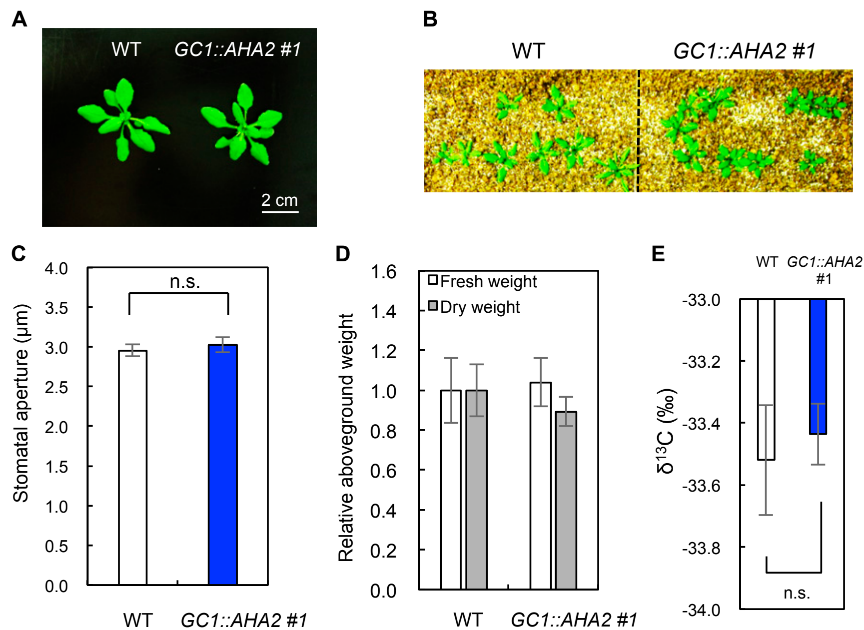

Fig. S6. Phenotypic characterization of *AHA2*-transgenic plants under mild drought conditions. WT and transgenic plants were grown in the same planter under normal water conditions (~80% soil water content) until germination. The soil water content was then decreased to 40–50% by reducing the number of waterings. (*A* and *B*) Phenotypes of WT and *AHA2*-transgenic plants grown under high light conditions (200 μmol·m^{-2}·s^{-1}) for 25 d. (*C*) Stomatal aperture under growth conditions (200 μmol·m^{-2}·s^{-1}). Error bars represent the SEM (n = 30). (*D*) Relative aboveground fresh and dry weights of 25-d-old plants. (*E*) Carbon isotope ratios (δ^{13}C) of WT and *AHA2*-transgenic plants. Error bars represent the SEM (n = 5). Significant differences in stomatal aperture were detected using Student t test. n.s., not significant (P > 0.05).

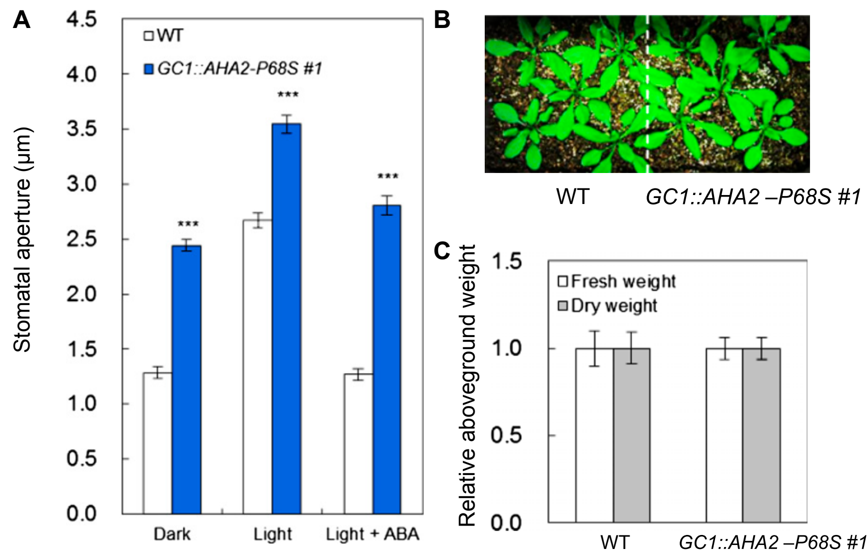

Fig. S7. Overexpression of *AHA2* with Pro68-to-Ser point mutation (*AHA2-P68S*) using the *GC1* promoter increases stomatal opening but not plant growth. (*A*) Stomatal apertures in plants grown under 2.5 h of darkness, light (50 μmol·m^{-2}·s^{-1} red light and 10 μmol·m^{-2}·s^{-1} blue light), or light in the presence of 20 μM ABA. (*B*) Phenotypes of WT and *AHA2-P68S*–transgenic plants (*GC1::AHA2-P68S*) grown under high light conditions (200 μmol·m^{-2}·s^{-1}) for 25 d. (*C*) Relative aboveground fresh and dry weights of 25-d-old plants. Fresh and dry weight values are the means of measurements of more than nine plants; error bars represent the SEM. Significant differences were detected by Student t test.

Table S1. Gas-exchange parameters of WT and *GC1::AHA2* transgenic plants

Parameters	WT	*GC1::AHA2* #1		*GC1::AHA2* #2	
Light intensity at 200 $\mu mol \cdot m^{-2} \cdot s^{-1}$					
CO_2 assimilation rate, $\mu mol \cdot m^{-2} \cdot s^{-1}$	4.34 ± 0.31	5.07 ± 0.16*	$P < 0.05$	4.95 ± 0.14*	$P < 0.05$
Stomatal conductance, $mol \cdot m^{-2} \cdot s^{-1}$	0.070 ± 0.003	0.099 ± 0.011†	$P < 0.005$	0.099 ± 0.012*	$P < 0.05$
Ci, $\mu L \cdot L^{-1}$	267.9 ± 5.8	283.6 ± 9.5*	$P < 0.05$	286.4 ± 11.5*	$P < 0.05$
Transpiration rate, $mmol \cdot m^{-2} \cdot s^{-1}$	1.33 ± 0.08	1.84 ± 0.22*	$P < 0.05$	1.74 ± 0.19*	$P < 0.05$
Water use efficiency	3.28 ± 0.37	2.79 ± 0.29	$P = 0.085$	2.88 ± 0.42	$P = 0.239$
Light intensity at 1,000 $\mu mol \cdot m^{-2} \cdot s^{-1}$					
CO_2 assimilation rate, $\mu mol \cdot m^{-2} \cdot s^{-1}$	5.08 ± 0.20	5.83 ± 0.25†	$P < 0.005$	5.88 ± 0.34*	$P < 0.05$
Stomatal conductance, $mol \cdot m^{-2} \cdot s^{-1}$	0.082 ± 0.002	0.134 ± 0.020†	$P < 0.005$	0.128 ± 0.029*	$P < 0.05$
Ci, $\mu L \cdot L^{-1}$	266.9 ± 1.6	294.9 ± 8.6‡	$P < 0.001$	289.3 ± 25.3	$P = 0.121$
Transpiration rate, $mmol \cdot m^{-2} \cdot s^{-1}$	1.58 ± 0.07	2.53 ± 0.49*	$P < 0.05$	2.24 ± 0.26†	$P < 0.005$
Water use efficiency	3.22 ± 0.19	2.36 ± 0.41*	$P < 0.05$	2.67 ± 0.47	$P = 0.082$

Measurements were conducted at 380 $\mu L \cdot L^{-1}$ CO_2. Water use efficiency was calculated as the ratio between CO_2 assimilation rate and transpiration rate. Differences were detected by Student *t* test; ± SD ($n \geq 3$). These parameters were concluded from light exposure curves, as plotted in Fig. 2 *A* and *B*. Statistically significant: *$P < 0.05$; †$P < 0.005$; ‡$P < 0.001$. Ci, intercellular CO_2 concentration.